Electronic Supplementary Material (ESI) for RSC Advances.

Support Information

Microstructural study of epoxy-based thermosets prepared by "classical" and cationic frontal polymerization.

Helena Švajdlenková,*[a,d] Angela Kleinová,[a] Ondrej Šauša,[b] Jaroslav Rusnák,[c] Tran Anh Dung,[d] Thomas Koch,[e] Patrick Knaack,*[d]

[a] Department of Synthesis and Characterization of Polymers, Polymer Institute of SAS, Dúbravská cesta 9, Bratislava 845 41, Slovakia

[b] Department of Nuclear Physics, Institute of Physics of SAS, Dúbravská cesta 9, Bratislava 845 11, Slovakia

[c] Department of Metal Physics, Institute of Physics of SAS, Dúbravská cesta 9, Bratislava 845 11, Slovakia

[d] Institute of Applied Synthetic Chemistry, TU Wien, Getreidemarkt 9/163 MC, 1060 Vienna, Austria

[e] Institute of Materials Science and Technology, TU Wien, Getreidemarkt 9/308, 1060 Vienna, Austria

*Corresponding authors: helena.svajdlenkova@savba.sk, patrick.knaack@tuwien.ac.at

"Classically" cured samples

- Photo- and thermally-cured epoxy samples (PCES, TCES)

  PCES samples were cured in the silicon mould with the geometry: diameter of 15 mm, thickness of 3 mm.

  TCES sample was cured in the cylindrical mould in the oven at 160 °C for 10 hours.

a) b)

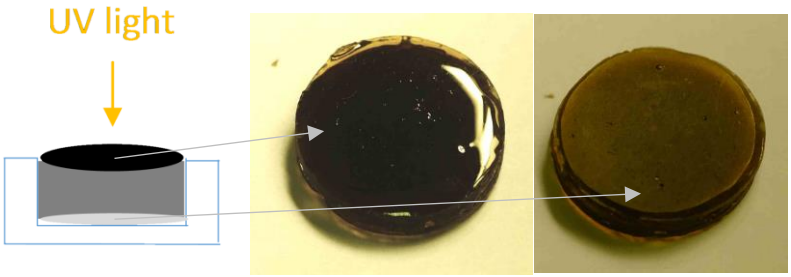

Fig. S1 a) The silicon mould for PCES samples. b) The shiny and matte side of the PCES samples cured in the UV light oven.

Fig. S2 Anhydride-based epoxy sample (TCES) was cut into 3mm thick discs.

The samples prepared by photo and thermal RICFP

The samples were cured in the Teflon cylindrical mould, which had three different bottom parts (Fig. S3). The cured samples were cut into 3 mm thick discs (Fig. S4). The temperature of the mould before the cationic frontal polymerization was around 27 °C.

Fig. S3 The schema of the experimental arrangement of the photo-induced RICFP by UV light. In the first picture, the reaction systems were triggered by UV light, which was passed through the thin SiO_2 glass plate fixed at the bottom of the mould. Next three pictures represent the Teflon cylindrical mould with three different bottom parts, i.e. the glassy plate, the Teflon plate with an integrated metal part in the middle used for a soldering iron, and the Al spacer used for a heating plate.

A/

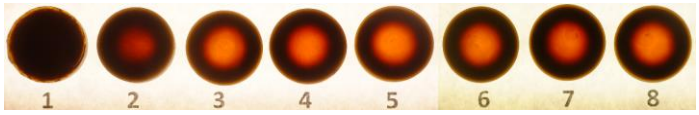

B/

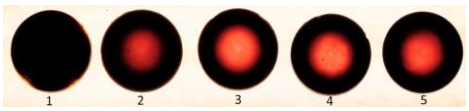

C/

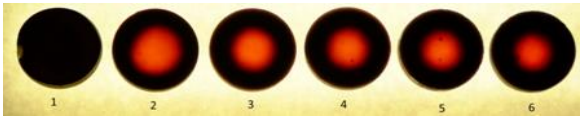

Fig. S4 Cut samples of photo RICFP sample - A, and of thermal RICFP samples triggered by the soldering iron- B and the heating plate - C.

The flux density profile of UV light was determined from the values measured with the step of 3 mm (Fig. S5) by Ophir Photonics StarLite meter with the probe PD300-UV.

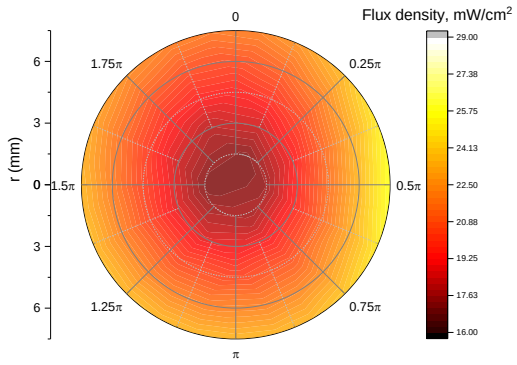

Fig. S5 The flux density profile of UV light.

Mould A and B

Two thermocouple (TC) systems A and B consisted of 6 or 7 TCs (Fig. S6). The TC system A had a pair of TCs (TC1, TC3) fixed 2 mm and 20 mm from the bottom of the mould. For the TC system B, TC2 was placed in the middle, between TC1 and TC3.

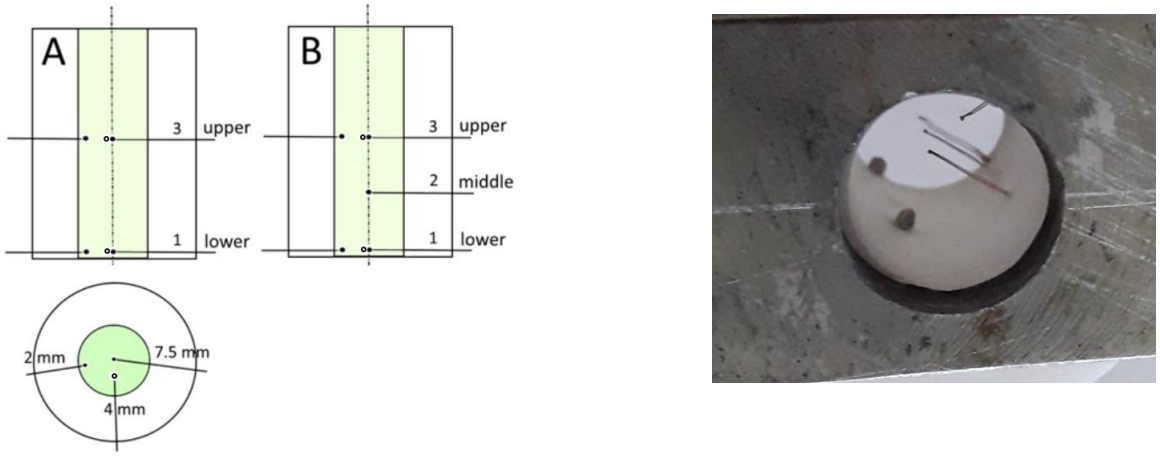

Fig. S6 The cylindrical mould with the positions of thermocouples (A, B). The internal diameter of the cylinder was 15 mm. The mould A consisted of two TCs (TC1, TC3), which had the distance 18 mm. TCs, immersed into reaction volume, were fixed at 7.5 mm, 4 mm and 2 mm from the inner surface of the cylinder mould. In the case of the mould B, an extra TC (TC2) was placed between lower and upper TCs (TC1, TC3).

Temperature profiles for the samples cured by photo and thermal RICFP

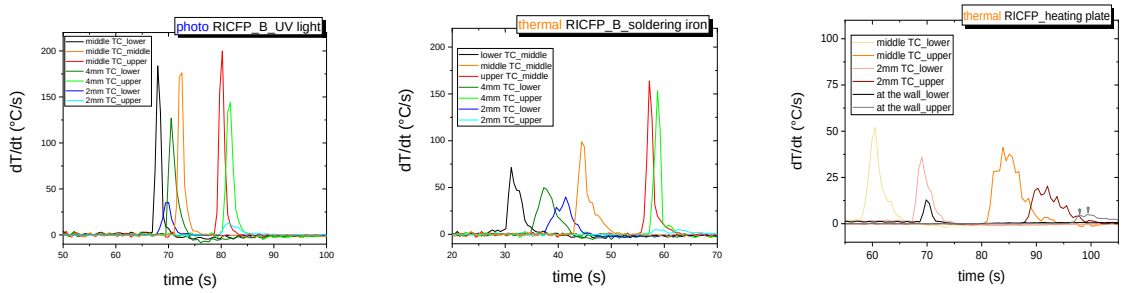

Fig. S7 The time derivative of the temperature profiles for photo- and thermally-induced RICFP.

The velocity at the inflection point (v_{ip}) were determined from the peak maximum of the time derivatives of the temperature profiles. These temperature profiles reflect the thermal effect during the frontal propagation.

ATR/FTIR

"Classically" thermally-cured BADGE+anhydrid + cat. (TCES)

ATR/FTIR data from

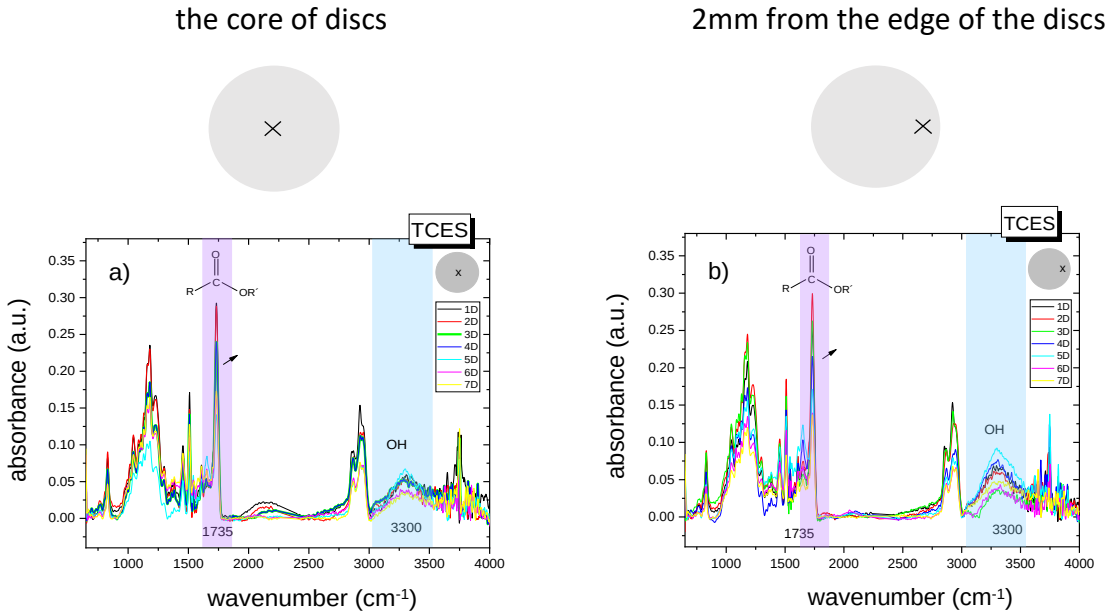

Fig. S8 ATR/FTIR spectral evolution of the TCES sample a) in the core and b) 2 mm from the edge of all discs.

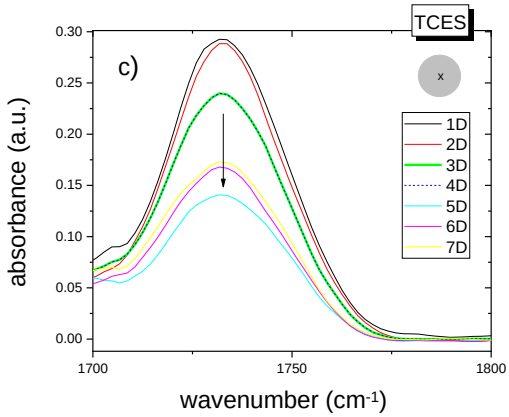

Fig. S8 c) The reduction of the intensity of carbonyl ester stretching band, (1735 cm^{-1}), in the core of discs, indicates stronger H bond interactions between O-H·····O=C. Arrow shows the trend of the evolution of the peak.

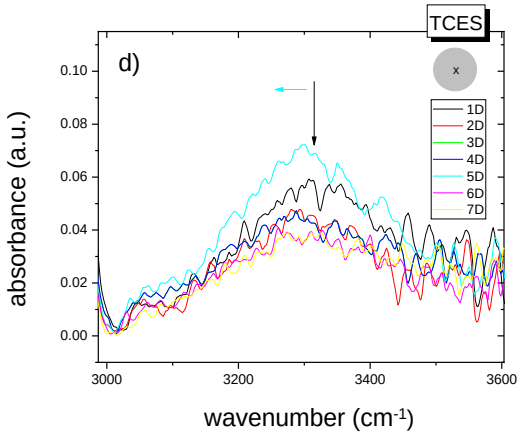

Fig. S8 d) The decrease of an OH absorption peak at 3200 – 3600 cm^{-1}, and its shift to the lower wavenumber, in the core of discs, implies the formation of a stronger complex of H bonds between OH groups and carbonyl groups O-H·····O=C. Arrows show the trend of the evolution of the peak.

"Classically" photo- cured epoxy sample (PCES)

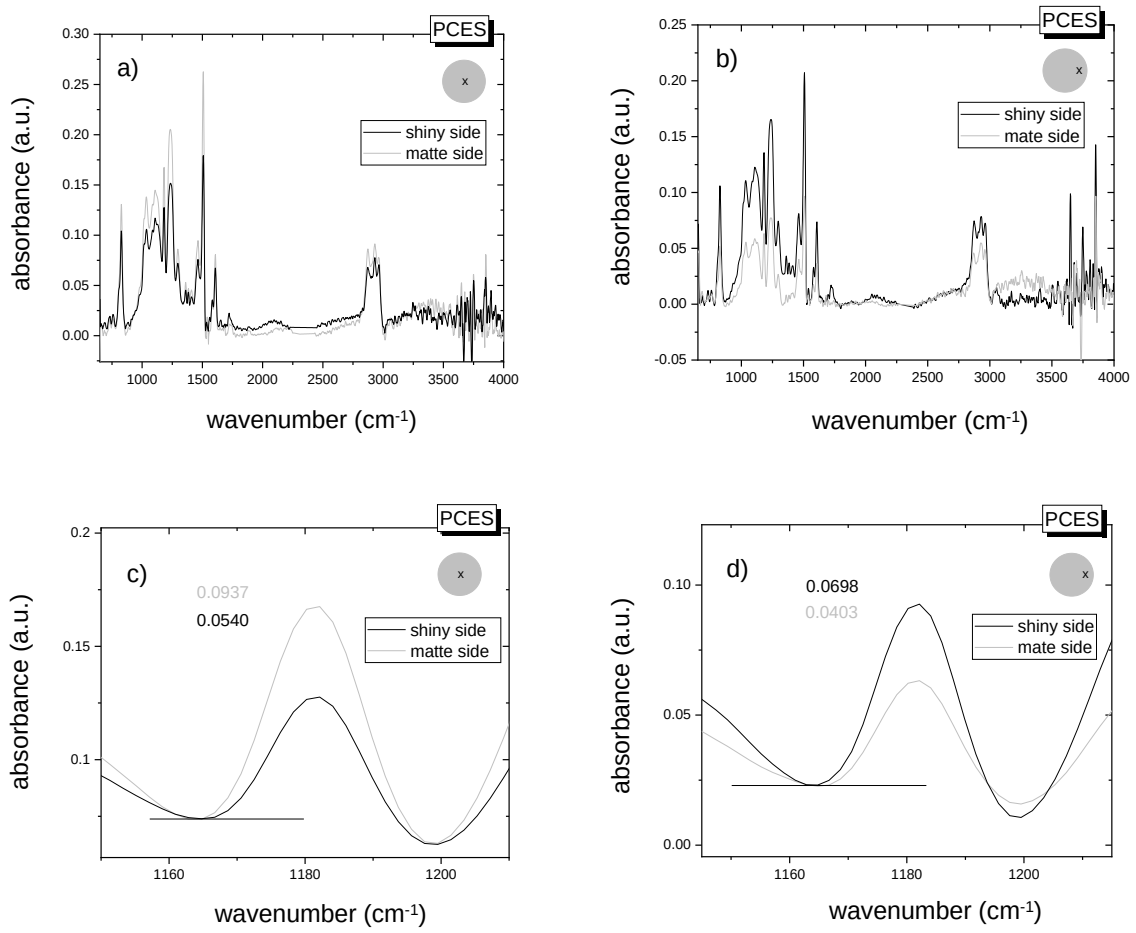

Fig. S9 ATR/FTIR spectrum of "classically" cured sample by UV light (PCES), the shiny side and the matte one, (a) in the core and (b) 2 mm from the edge of the disc. The amplitude of ether groups (1182 cm^{-1}) was determined for the shiny and the matte side (c) in the core of the disc and (d) 2 mm from the edge of the disc.

Photo RICFP induced by UV light

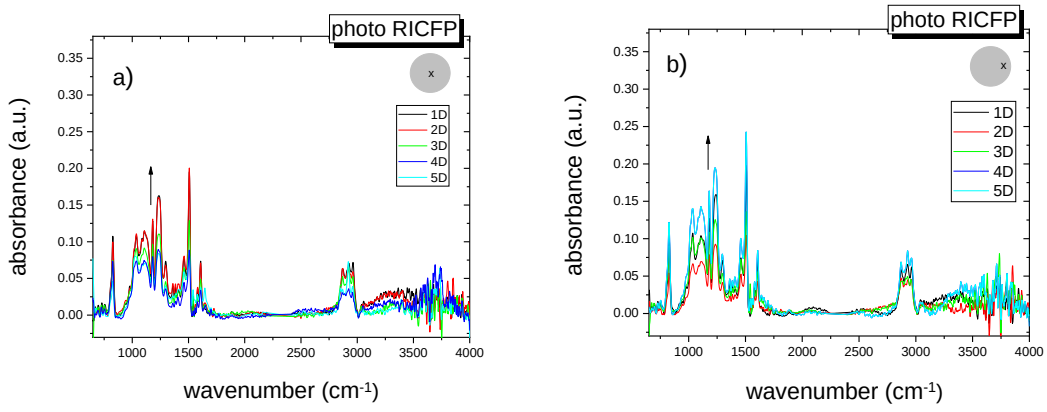

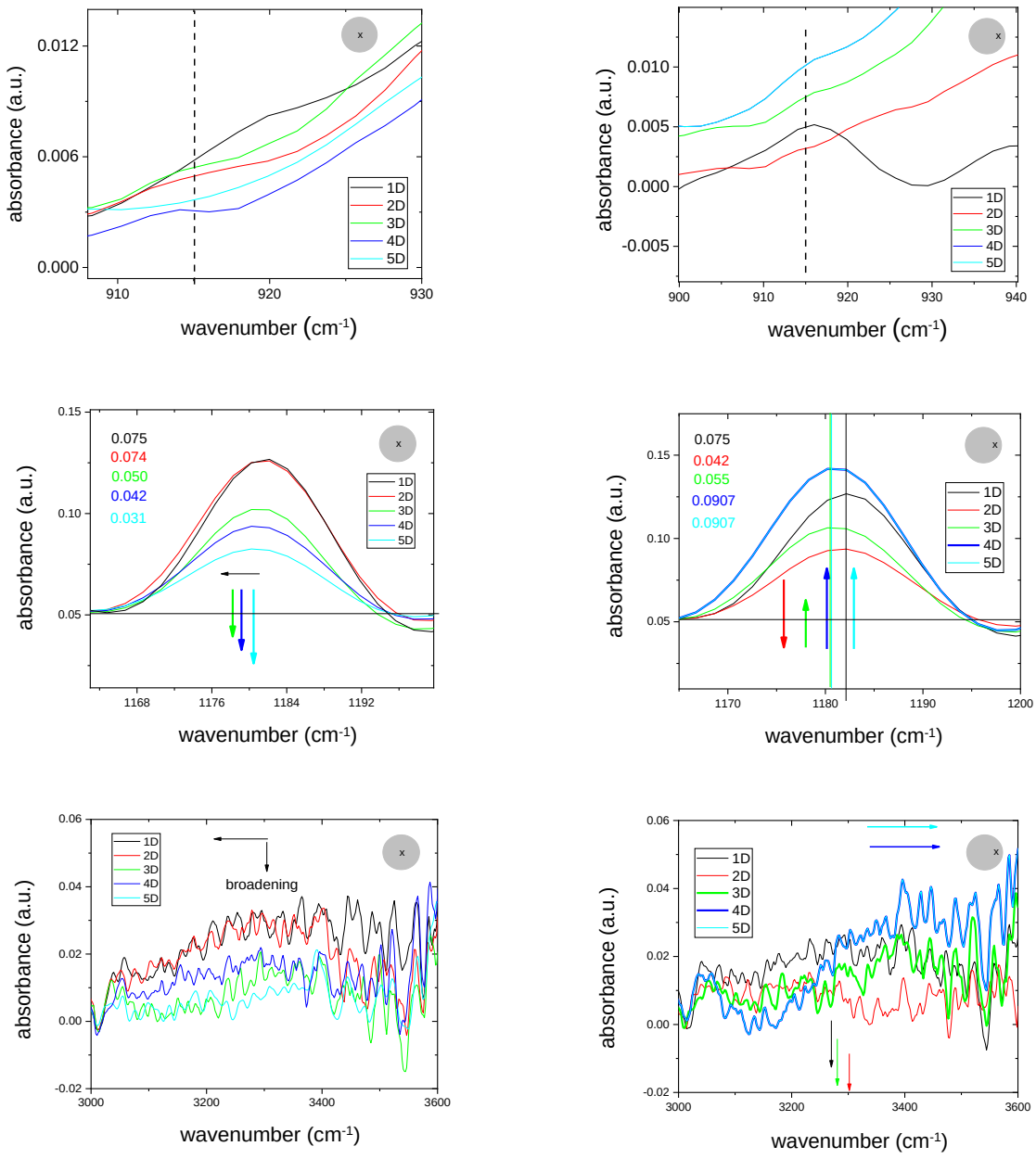

Fig. S10 ATR/FTIR spectral evolution of the photo RICFP sample a) in the core and b) 2 mm from the edge of all discs. The amplitudes of bands were determined for ether groups (1182 cm^{-1}) and OH groups in the range of 3000 – 3600 cm^{-1}. Arrows show the trend of the evolution of both peaks.

Thermal RICFP induced by the soldering iron

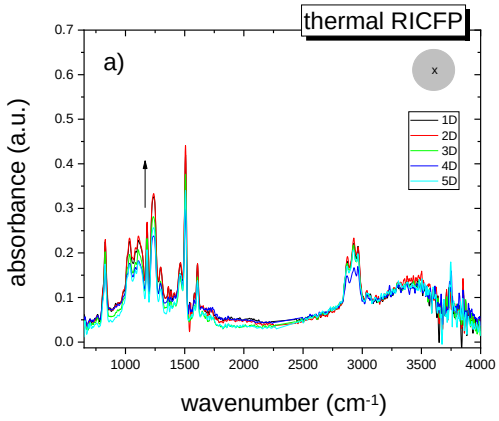
thermal RICFP
a)
1D
2D
3D
4D
5D
absorbance (a.u.)
wavenumber (cm-1)

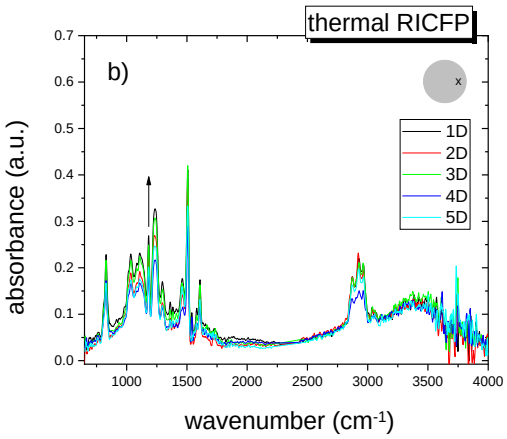
thermal RICFP
b)
1D
2D
3D
4D
5D
absorbance (a.u.)
wavenumber (cm-1)

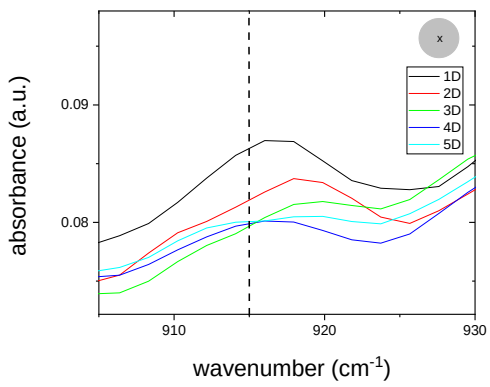
1D
2D
3D
4D
5D
absorbance (a.u.)
wavenumber (cm-1)

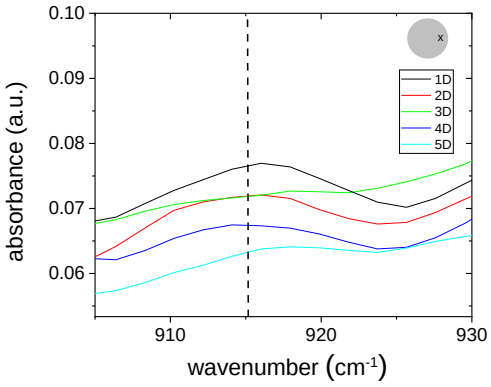
1D
2D
3D
4D
5D
absorbance (a.u.)
wavenumber (cm-1)

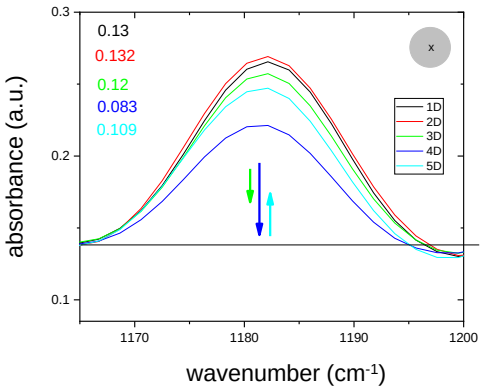
0.13
0.132
0.12
0.083
0.109
1D
2D
3D
4D
5D
absorbance (a.u.)
wavenumber (cm-1)

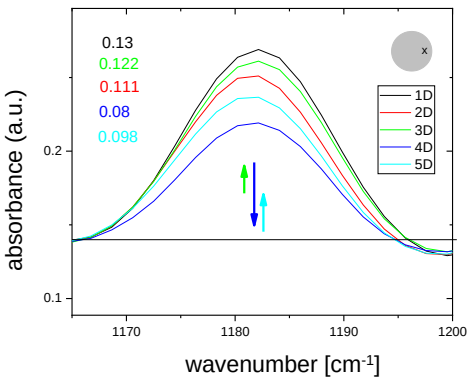
0.13
0.122
0.111
0.08
0.098
1D
2D
3D
4D
5D
absorbance (a.u.)
wavenumber [cm-1]

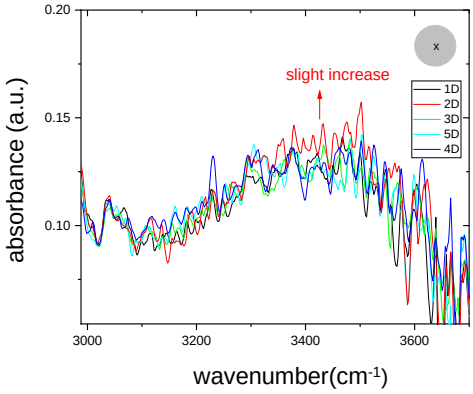
slight increase
1D
2D
3D
5D
4D
absorbance (a.u.)
wavenumber(cm-1)

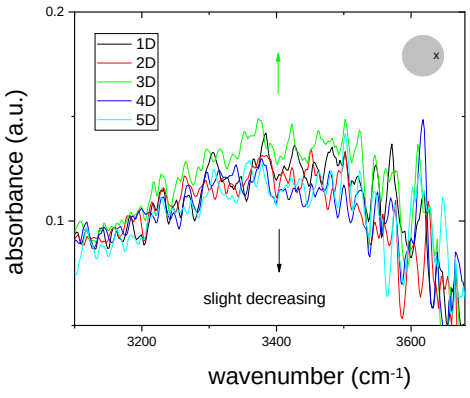
1D
2D
3D
4D
5D
slight decreasing
absorbance (a.u.)
wavenumber (cm-1)

Fig. S11 ATR/FTIR spectral evolution of the thermal RICFP sample a) in the core and b) 2 mm from the edge of all discs. The amplitudes of bands were determined for ether groups (1182 cm^{-1}) and OH groups in the range of 3000 – 3600 cm^{-1}. Arrows show the trend of the evolution of both peaks.

The conversion of monomers, which is reflected by the disappearance of the oxirane group, i.e. C-O group (915 cm^{-1}), showed higher conversion of monomers in the in photo RICFP sample than in thermal RICFP one (Fig. S10, and S11 a, b).

PALS measurement of angular profile

The epoxy resins cured by photo- and thermally-induced RICFP

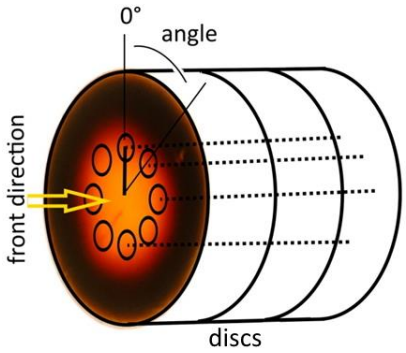

Fig. S12 The schema of angular measurement for 1st until 4th discs at a constant radius of 3 mm. The started point, i.e. zero angle, was marked by the line on the surface of the cylindrical samples.

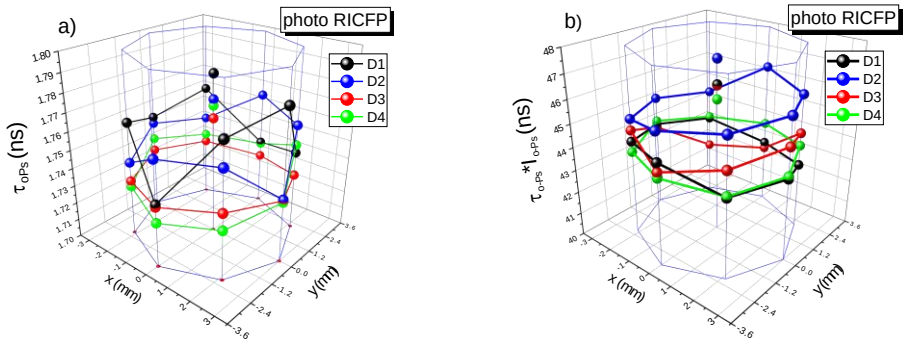

Fig. S13 The 3D angular dependence a) of *o*-Ps lifetime and b) $\tau_{o\text{-}Ps}*I_{o\text{-}Ps}$ for the discs D1-D4 of photo-RICFP sample. Both values were determined 3 mm from the edge and in the core of discs.

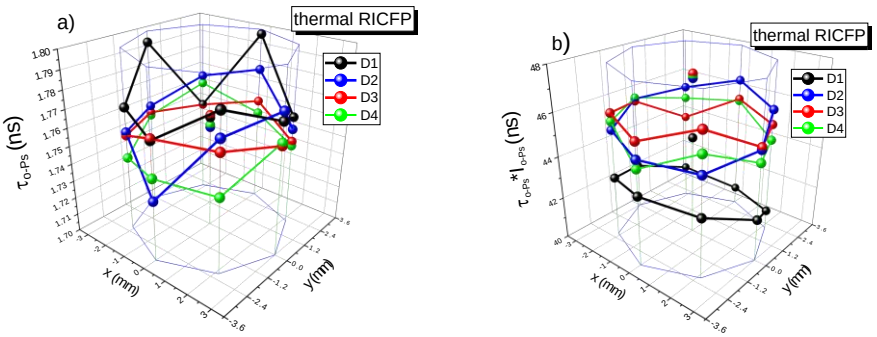

Fig. S14 The 3D angular dependence of a) *o*-Ps lifetime and b) $\tau_{o\text{-}Ps}$*$I_{o\text{-}Ps}$ for the discs D1-D4 of thermal RICFP sample.-Both values were determined 3 mm from the edge and in the core of discs.

Angular dependences were measured for photo and thermal RICFP samples, according to the scheme in Fig. S12. The 3D plots of the *o*-Ps lifetime and $\tau_{o\text{-}Ps}$ * $I_{o\text{-}Ps}$ (free volume fraction parameter) are displayed in the Figures S13 and S14. The 1st discs (D1) showed significant differences in *o*-Ps lifetimes for both samples. Other discs exhibited a gradual reduction of the *o*-Ps lifetime oscillation. The angular dependence of $\tau_{o\text{-}Ps}$ * $I_{o\text{-}Ps}$ displayed values without oscillation for D1.

However, thermal RICFP triggered by the point heat source probably caused axial and radial movements of the frontal waves, simultaneously. This can lead to the stronger angular dependence of the fraction and its low value in D1.

"Classically" thermally-cured BADGE+anhydrid + cat. (TCES)

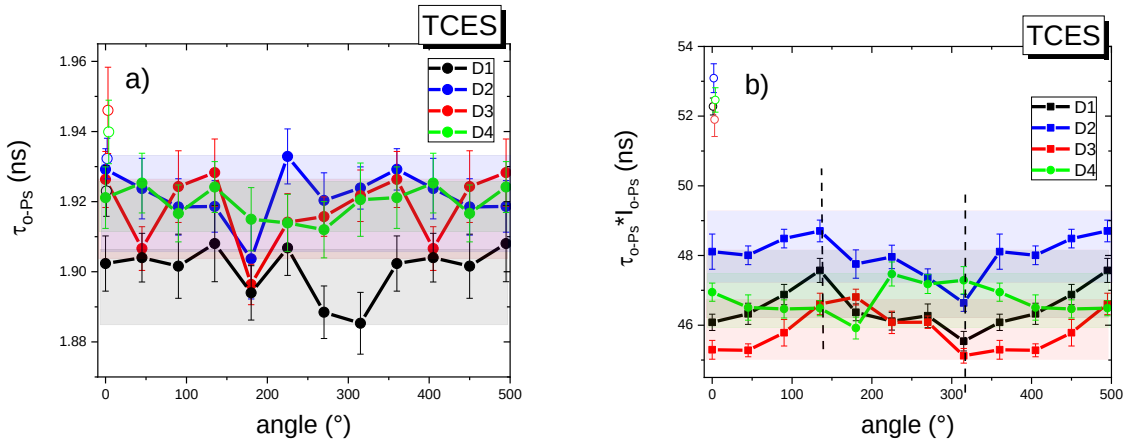

Fig. S15 The 2D angular dependence of a) *o*-Ps lifetime and b) $\tau_{o\text{-}Ps}*I_{o\text{-}Ps}$ for the discs D1-D3 of thermally cured TCES sample. Both values were determined 3 mm from the edge of discs (full symbols) and in the core of discs (open symbols).

In the Fig. S15 and S16, the angular dependences of $\tau_{o\text{-}Ps}$ and $\tau_{o\text{-}Ps}*I_{o\text{-}Ps}$ are displayed for "classically" cured anhydride-based sample (TCES). The sizes of holes are larger than in the RICFP-based samples. There is no evidence about the angular movement of local free volume fractions between discs.

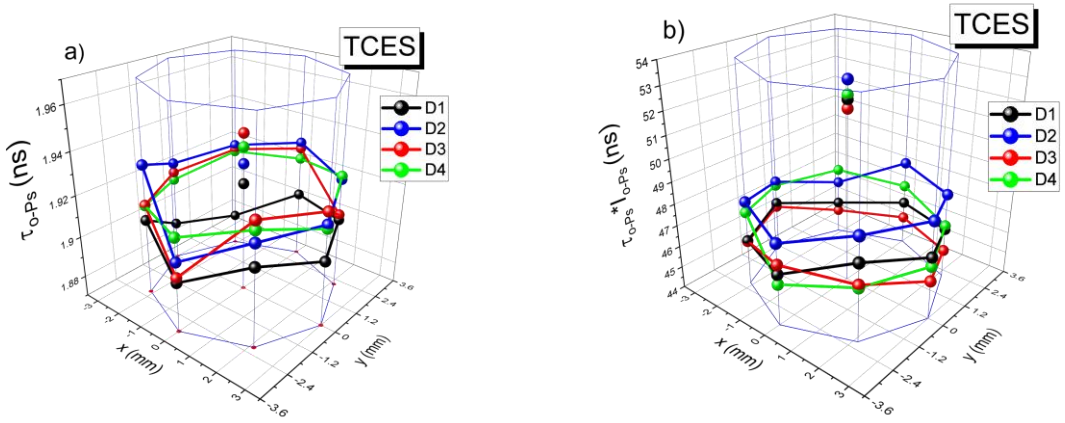

Fig. S16 The 3D angular dependence of a) *o*-Ps lifetime and b) $\tau_{o\text{-}Ps}*I_{o\text{-}Ps}$ for the discs D1-D3 of the thermally-cured TCES sample. Both values were determined 3 mm from the edge and in the core of discs.